DOI: https://doi.org/10.15407/techned2020.03.022

EFFECT OF ELECTRIC CONDUCTING ELEMENT ON INDICATORS OF LINEAR PULSE ELECTROMECHANICAL CONVERTER INDUCTION TYPE

V.F. Bolyukh*
National Technical University "Kharkiv Polytechnic Institute",
st. Kirpicheva, 2, Kharkov, 61002, Ukraine,
e-mail: vfbolyukh@gmail.com

The purpose of the article is to study the influence of geometric parameters and the location of a coaxially located electrically conductive element (ECE), made in the form of a thin-walled disk, ring or hollow cylinder, on the characteristics and performance of an induction-type linear pulse electromechanical converter (LPEC). A mathematical model has been developed that describes the electromechanical and thermal processes in an induction-type LPEC using the concentrated parameters of active elements. It is shown that the ECE, coaxially mounted near the inductor winding, has a negative effect on the performance of the LPEC. The smallest value of the converter efficiency of 6.1% occurs when ECE is used in the form of a thin copper disk 0.5 mm high, in which the radial dimensions are similar to the sizes of the windings of the inductor and the armature installed at a minimum distance from the inductor. Moreover, the temperature rise of the electrically conductive element is maximum and equal to 51°C. With an increase in the thickness of the ECE and with its removal from the inductor, the efficiency of the LPEC increases, and the excess of the temperature of the ECE decreases. When removing a disk ECE with a height of 1.0 mm at a distance of 10 mm from the inductor, the efficiency of the LPEC is 12.6%, and the excess of the ECE temperature is 6 °C. References 14, figures 6.
Key words: linear pulse electromechanical converter of induction type, electrically conductive element, mathematical model, electromechanical and thermal processes and indicators.

Introduction. Linear pulse electromechanical converters (LPEC) are designed to accelerate the actuator to high speed in a short section or to create powerful power pulses. LPECs are used in many branches of science, engineering and technology as electromechanical accelerators and shock-force devices. In construction, electromagnetic hammers and perforators are used, in the mining industry - butters and vibrators, in geological exploration – vibration sources, in mechanical engineering - hammers with a large range of impact energy and devices for electrodynamics' processing of welded joints, in the chemical and biomedical industry – vibration mixers, etc. [7–9, 12]. LPECs are used in test complexes for testing critical equipment for impact loads, in high-speed electric devices, in magnetic pulse devices for pressing ceramic powders, for cleaning containers from sticking bulk materials, as a catapult for ballistic gravimeters or launching unmanned aerial vehicles, in devices ultrafast cooling of biological objects, etc. [3, 5, 6, 10].

The most widely used are LPECs of induction type, which, as a rule, have a coaxial configuration and are excited from a capacitive energy storage device (CESD) [2, 4]. In the design of such a converter there are various elements that ensure its functioning: support, mounting, guides, return, shielding, protective, etc. [1, 4, 14, 13]. These metal elements, as a rule, influence the performance and performance of an induction-type LPEC. A particularly strong effect arises when the electrically conductive element is located near the LIEC inductor. However, the influence of both the geometric parameters of the specified electrically conductive element (ECE) and its relative position relative to the inductor has not been studied.

The purpose of the article is to determine the influence of geometric parameters and the location of a coaxially located electrically conductive element, made in the form of a thin-walled disk, ring or hollow cylinder, on the characteristics and performance of an induction-type LPEC.

Mathematical model of LPEC. Consider the constructive scheme of an induction-type LPEC containing active elements: a fixed inductor *1*, an accelerated armature *2*, and an electrically conductive element *3* (Fig. 1). An armature provides movement of the actuator *4* along the *z* axis. The inductor is made in the form of a multi-turn winding connected to the CESD. The armature is made in the form of a multi-turn short-circuited winding. ECE 3 is made in

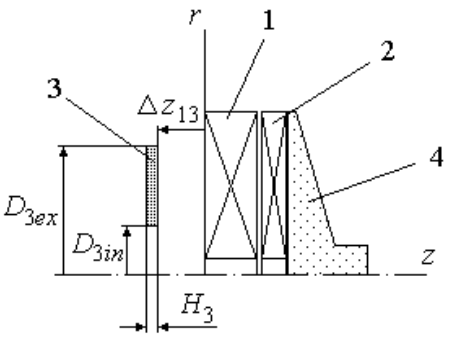

Fig. 1

*ORCID: https://orcid.org/0000-0001-9115-7828

the form of a thin-walled disk, ring or hollow cylinder made of conductive material. ECE is coaxially located relative to the inductor at a distance Δz_{13} and is made with external D_{3ex} and internal D_{3in} diameters and axial height H_3.

We assume that the coaxially mounted fixed inductor and accelerated armature contain multi-turn disk windings that are tightly wound in two rows of copper bus. Consider a mathematical model of an induction type LPEC, in which the concentrated parameters of the active elements are used - the fixed winding of the inductor (WI), the moving winding of the armature (WA) and the stationary ECE. The chain model makes it possible to quickly calculate the LPEC indicators while varying various parameters and the location of the ECE [11]. Consider a mathematical model that describes electromagnetic processes in an induction-type LPEC using lumped parameters of active elements:

$$i_1R_1(T_1)+L_1\frac{di_1}{dt}+u_c+M_{12}(z)\frac{di_2}{dt}+M_{13}\frac{di_3}{dt}+v_2(t)i_2\frac{dM_{12}}{dz}=0;\ \ u_c=U_0+\frac{1}{C}\int_0^t i_1dt; \tag{1}$$

$$i_2R_2(T_2)+L_2\frac{di_2}{dt}+M_{12}(z)\frac{di_1}{dt}+M_{23}(z)\frac{di_3}{dt}+v_2(t)\left(i_1\frac{dM_{12}}{dz}+i_3\frac{dM_{23}}{dz}\right)=0; \tag{2}$$

$$i_3R_3(T_3)+L_3\frac{di_3}{dt}+M_{13}\frac{di_1}{dt}+M_{23}(z)\frac{di_2}{dt}+i_2v_2(t)\frac{dM_{23}}{dz}=0, \tag{3}$$

where p=1, 2, 3 are the indices of WI, WA and ECE, respectively; $R_p(T_p)$, L_p, i_p, T_p are the resistance, inductance, current and temperature of the p^{th} active element, respectively; $M_{12}(z)$, M_{13}, $M_{23}(z)$ are the mutual inductances between the corresponding p^{th} active elements; $v_2(t)$ is the velocity of the WA relative to the WI along the z axis.

The joint solution of equations (1) – (3) after a series of transformations allows us to reduce them to a single differential equation (for fixed values of the parameters $R_p(T_p)$, $M_{12}(z)$, $M_{23}(z)$ и $v_2(t)$):

$$a_4\frac{d^4i_1}{dt^4}+a_3\frac{d^3i_1}{dt^3}+a_2\frac{d^2i_1}{dt^2}+a_1\frac{di_1}{dt}+a_0=0, \tag{4}$$

where $a_0=C^{-1}\left(R_2R_3-\vartheta_{23}^2\right)$; $a_1=R_1\left(R_2R_3-\vartheta_{23}^2\right)-R_3\vartheta_{12}^2+C^{-1}\left(R_2L_3+R_3L_2-2M_{23}\vartheta_{23}\right)$;

$a_2=\iota_{23}C^{-1}+L_1\left(R_2R_3-\vartheta_{23}^2\right)+L_2R_1R_3+L_3\left(R_1R_2-\vartheta_{12}^2\right)+2\left[\vartheta_{12}\left(M_{13}\vartheta_{23}-M_{12}R_3\right)-M_{23}R_1\vartheta_{23}\right]$;

$a_3=\iota_{23}R_1+\iota_{13}R_2+\iota_{12}R_3+2\vartheta_{23}\varepsilon_1+2\vartheta_{12}\varepsilon_3$; $a_4=\iota_{23}L_1+M_{13}\varepsilon_2+M_{12}\varepsilon_3$; $\iota_{23}=L_2L_3-M_{23}^2$;

$\iota_{13}=L_1L_3-M_{13}^2$; $\iota_{12}=L_1L_2-M_{12}^2$; $\varepsilon_1=M_{12}M_{13}-L_1M_{23}$; $\varepsilon_2=M_{12}M_{23}-L_2M_{13}$; $\varepsilon_3=M_{13}M_{23}-L_3M_{12}$;

$\vartheta_{12}=v_2\frac{dM_{12}}{dz}$; $\vartheta_{23}=v_2\frac{dM_{23}}{dz}$.

The characteristic equation of the differential equation (4)

$$a_4x^4+a_3x^3+a_2x^2+a_1x+a_0=0 \tag{5}$$

by means of a replacement $\varpi=x+0,25a_3/a_4$ it is translated into the reduced form with a cubic resolvent:

$$\varpi^3+q_1\cdot\varpi^2+q_2\cdot\varpi-q_3^2=0, \tag{6}$$

where $q_1=2\frac{a_2}{a_4}-0,75\left(\frac{a_3}{a_4}\right)^2$; $q_2=3\left(\frac{a_3}{2\cdot a_4}\right)^4-\frac{a_3^2\cdot a_2}{a_4^3}+\frac{a_1\cdot a_3+a_2^2}{a_4^2}-4\frac{a_0}{a_4}$;

$q_3=\left(\frac{a_3}{2\cdot a_4}\right)^3-0,5\frac{a_2\cdot a_3}{a_4^2}+\frac{a_1}{a_4}$.

If the discriminate is resolvent

$$D=(\varsigma/3)^3-(\upsilon/2)^2, \tag{7}$$

where $\varsigma=q_2-q_1^2/3$; $\upsilon=2\cdot q_1^3/27-q_1\cdot q_2/3-q_3^2$, less than zero, then using the trigonometric solution of equation (6), we get:

$$\varpi_p=2\cdot\sqrt[3]{\left(-\frac{\varsigma^3}{27}\right)^{0,5}}\cos\left(\frac{2\pi(p-1)}{3}+\frac{\arccos\left(-0,5\upsilon\sqrt{-27/a_3^3}\right)}{3}\right). \tag{8}$$

In this case, the roots of equation (5) are equal to:

$$x_l = 0{,}5 \cdot \left(\pm \sqrt{\varpi_1} \pm \sqrt{\varpi_2} \pm \sqrt{\varpi_3} \right) - 0{,}25 \cdot a_3 / a_4 , \tag{9}$$

where l=1, 2, 3, 4.

If all the roots (9) are real, then for the currents in the p^{th} active elements of the LPEC you can write:

$$i_p = \frac{U_0}{a_4} \frac{A_{p1} \exp(x_1 t) + A_{p2} \exp(x_2 t) + A_{p3} \exp(x_3 t) + A_{p4} \exp(x_4 t)}{\gamma_{21}\gamma_{43}(\delta_{21} + \delta_{43}) + \gamma_{24}\gamma_{31}(\delta_{24} + \delta_{31}) + \gamma_{32}\gamma_{41}(\delta_{32} + \delta_{41})}, \tag{10}$$

where $A_{p1} = \gamma_{32}(\alpha_4 - \Theta_p \delta_{32}) + \gamma_{24}(\alpha_3 - \Theta_p \delta_{24}) + \gamma_{43}(\alpha_2 - \Theta_p \delta_{43})$;

$A_{p2} = \gamma_{13}(\alpha_2 - \Theta_p \delta_{13}) + \gamma_{41}(\alpha_3 - \Theta_p \delta_{41}) + \gamma_{34}(\alpha_1 - \Theta_p \delta_{34})$;

$A_{p3} = \gamma_{21}(\alpha_4 - \Theta_p \delta_{21}) + \gamma_{42}(\alpha_1 - \Theta_p \delta_{42}) + \gamma_{14}(\alpha_2 - \Theta_p \delta_{14})$;

$A_{p4} = \gamma_{12}(\alpha_3 - \Theta_p \delta_{12}) + \gamma_{31}(\alpha_2 - \Theta_p \delta_{31}) + \gamma_{23}(\alpha_1 - \Theta_p \delta_{23})$;

$\gamma_{kl} = x_k - x_l$; $\alpha_k = (\Lambda_p x_k - \Xi_p) x_k^2$; $\delta_{kl} = x_k^2 x_l^2$; $\Theta_1 = -\iota_{23}$; $\Theta_n = -\varepsilon_m$; $\Lambda_1 = \zeta_1 / a_4$; $\Lambda_n = \zeta_n / a_4$;

$\Xi_1 = \left[a_4 \iota_{23}^2 / C - \zeta_1 (R_1 \iota_{23} + \vartheta_{12} \varepsilon_3) - \zeta_2 (R_2 \varepsilon_3 + \vartheta_{12} \iota_{23} + \vartheta_{23} \varepsilon_2) - \zeta_3 (R_3 \varepsilon_2 + \vartheta_{23} \varepsilon_3) \right] / a_4^2$;

$\Xi_n = \left[a_4 \iota_{23} \varepsilon_m / C - \zeta_1 (R_1 \varepsilon_m + \vartheta_m \iota_n + \vartheta_n \varepsilon_1) - \zeta_n (R_n \iota_n + \vartheta_m \varepsilon_m + \vartheta_{23} \varepsilon_1) - \zeta_m (R_m \varepsilon_1 + \vartheta_n \varepsilon_m + \vartheta_1 \iota_n) \right] / a_4^2$;

$\zeta_1 = R_1 \iota_{23}^2 + R_2 \varepsilon_3^2 + R_3 \varepsilon_2^2 + 2[\iota_{23} \vartheta_{12} \varepsilon_3 + \vartheta_{23} \varepsilon_2 \varepsilon_3]$;

$\zeta_n = \varepsilon_m (R_1 \iota_{23} + R_n \iota_n) + R_m \varepsilon_1 \varepsilon_n + \vartheta_m (\iota_{23} \iota_n + \varepsilon_m^2) - (\vartheta_n \iota_{23} + \vartheta_{23} \varepsilon_m) L_1 M_{nm} - L_n M_{1m} (\vartheta_n \varepsilon_m + \vartheta_{23} \iota_n) - L_m M_{1n} (\vartheta_{23} \varepsilon_1 + \vartheta_n \varepsilon_n)$.

$n = 2, 3$; $m = 5 - n$; $\vartheta_{13} = 0$.

If the discriminant of resolvent (7) is greater than zero, then using the Cardano solution for equation (6), we get one real and two complex conjugate roots:

$$\varpi_1 = \varphi + \zeta - q_1 / 3 ; \ \varpi_{2,3} = \delta \pm j\chi , \tag{11}$$

where $\phi = \sqrt[3]{-0{,}5\upsilon + \sqrt{D}}$; $\zeta = \sqrt[3]{-0{,}5\upsilon - \sqrt{D}}$; $\delta = -0{,}5 \cdot (\phi + \zeta) - q_1 / 3$; $\chi = 0{,}5 \cdot \sqrt{3} (\phi - \zeta)$.

In this case, the roots of equation (5) have the form:

$$x_{1,2} = 0{,}5 \cdot \sqrt{\varpi_1} - 0{,}25 \cdot a_3 / a_4 \pm \sqrt{0{,}5 \cdot \left(\delta + \sqrt{\delta^2 + \chi^2} \right)} ; \quad x_{3,4} = \sigma \pm j\xi , \tag{12}$$

where $\sigma = 0{,}5 \cdot \sqrt{\varpi_1} - 0{,}25 \cdot a_3 / a_4$; $\xi = \sqrt{0{,}5 \cdot \left(-\delta + \sqrt{\delta^2 + \chi^2} \right)}$.

If x_1 and x_2 are real and different, then the currents in the p^{th} active elements can be represented as:

$$i_p = \frac{U_0}{a_4} \frac{B_{p1} \exp(x_1 t) + B_{p2} \exp(x_2 t) + \exp(\sigma \cdot t) \left[B_{p3} \cos(\xi t) + B_{p4} \sin(\xi t) \right]}{x_1 x_2 (3\sigma^2 - 2\sigma\chi_1 - \xi^2 + x_1 x_2) + \chi_2 (\chi_2 + \chi_3 - 2\sigma\chi_1)} , \tag{13}$$

where $B_{p1} = \left\{ \Theta_p \left[x_2^2 (3\sigma^2 - \xi^2 - 2x_2\sigma) - \chi_2^2 \right] + \Lambda_p \left[2\sigma\chi_2 - x_2 (3\sigma^2 - \xi^2 - x_2^2) \right] - \Xi_p \left[(\sigma - x_2)^2 + \xi^2 \right] \right\} / (x_2 - \xi)$;

$B_{p2} = \left\{ \Theta_p \left[\chi_2^2 + \sigma^2 (\xi^2 - 3\sigma^2 + 2x_1\sigma) \right] + \Lambda_p \left[x_1 (3\sigma^2 - \xi^2) - 2\sigma\chi_2 \right] + \Xi_p (\chi_2 - 2x_1\sigma) \right\} / (x_2 - \xi)$;

$B_{p3} = \Theta_p \left[(\xi^2 - 3\sigma^2) \chi_1 + 2\sigma\chi_3 \right] + \Lambda_p \left[(3\sigma^2 - \xi^2) - \chi_3 \right] + \Xi_p (\chi_1 - 2\sigma)$;

$B_{p4} = \left\{ \Theta_p \left[\chi_3 (\xi^2 - \sigma^2) + \chi_1 \sigma (\sigma^2 - 3\xi^2) + x_1^2 x_2^2 \right] + \Lambda_p (\chi_3 \sigma - x_1 x_2 \chi_1 + 3\sigma\xi^2 - \sigma^3) + \Xi_p (\sigma^2 - \xi^2 + x_1 x_2 - \sigma\xi_1) \right\} / \xi$;

$\chi_1 = x_1 + x_2$; $\chi_2 = \sigma^2 + \xi^2$; $\chi_3 = x_1^2 + x_1 x_2 + x_2^2$.

The movement of the armature relative to the inductor can be represented as a recurrence relation:

$$h_2(t_{k+1}) = h_2(t_k) + v_2(t_k)\Delta t + \frac{\Delta t^2}{2(m_2 + m_e)} \left[\left(i_1(t_k) \frac{dM_{12}}{dz} + i_3(t_k) \frac{dM_{23}}{dz} \right) i_2(t_k) - K_T v_2(t_k) - \right.$$

$$\left. - 0{,}125 \cdot \pi \cdot \beta_a \gamma_a D_{2m}^2 v(t_k)^2 - K_P h_2(t_k) \right] , \tag{14}$$

where m_2, m_e are the mass of the inductor and actuator, respectively; v_2 is the speed of movement of the armature relative to the inductor; K_{P} is the coefficient of elasticity of the return element (spring); K_{T} is the coefficient of dynamic friction; γ_{a} is the density of the moving medium; β_{a} is the drag coefficient; $D_{2\text{m}}$ is the largest outer diameter of the WA or actuator; $\Delta t = t_{k+1} - t_k$ is the calculated time step.

The temperature of the p^{th} active element in the absence of thermal contact between them can be described by the recurrence relation [7]:

$$T_p(t_{k+1}) = T_p(t_k)\chi^* + \left(1-\chi^*\right)\left[T_0 + 4\pi^{-2} i_p^2(t_k) R_p(T_n)\alpha_{Tp}^{-1} D_{pex}^{-1} H_p^{-1}\left(D_{pex}^2 - D_{pin}^2\right)^{-1}\right], \quad (15)$$

where $\chi^* = \exp\left\{-0{,}25\Delta t D_{pex}\alpha_{Tp} c_p^{-1}(T_p)\gamma_p^{-1}\right\}$; D_{pex}, D_{pin} are the outer and inner diameters of the p^{th} active element, respectively; α_{Tp} is the heat transfer coefficient of the p^{th} active element; c_p is the heat capacity of the p^{th} active element.

The initial conditions of the mathematical model: $T_p(0)=T_0$ is the temperature of the p^{th} active element; $i_p(0)=0$ is the current of the p^{th} active element; $u_c(0)=U_0$ is the charge voltage of the CESD; Δz_0=1 mm is the distance between the WI and WA; $v_2(0)=0$ is the velocity of the armature along the z axis.

We will evaluate the efficiency of the induction-type LPEC with the following indicators: the largest instantaneous value f_{zm} of electrodynamic forces (EDF) – "EDF f_{zm}" and the largest impulse value F_z EDF – "EDF F_z", the highest values of armature speed v_2 and efficiency η with minimal excess temperatures of the p^{th} active elements θ_p. Instantaneous value of EDF acting on WA:

$$f_z(z,t) = i_2(z)\left(i_1(t)\frac{dM_{12}}{dz}(z) + i_3\frac{dM_{23}}{dz}(z)\right);\ F_z = \int_0^t f_z(z,t)dt;\ \eta = \left[\left(m_2+m_a\right)v_2^2 + K_P h_2^2\right]C^{-1}U_0^{-2};\ \theta_p = T_p - T_0.$$

Efficiency η is the ratio of mechanical energy to the initial energy of the CESD $W_0 = 0{,}5CU_0^2$. The mechanical energy developed by the converter consists of the kinetic energy of the moving elements (armature and actuator) $W_{kin} = 0{,}5(m_2+m_a)v_2^2(t)$ and the compression energy of the return spring $W_{pr} = 0{,}5K_P h_2^2(t)$.

Let us consider the LPEC in which the WI (p=1) is tightly wound with a copper busbar section $a_1\times b_1$= 4.8×1.8 mm^2, and the WA (p=2) is tightly wound with a copper busbar section $a_2\times b_2$= 1,4×0,9 mm^2. WI and WA are made with the same radial dimensions: outer diameter $D_{1ex}=D_{2ex}$=100 mm, inner diameter $D_{1in}=D_{2in}$=10 mm. The axial height of the WI is H_1=10 mm, and axial height of the WA is H_2=3 mm. CESD has the following parameters: capacitance C=250 μF, voltage U_0=3 kV. The coefficient of elasticity of the return spring K_P=25 kN/m. The mass of the actuating element m_a=0.25 kg. We will consider electromagnetic processes in the case of a free discharge of a CESD at WI.

Electromechanical indicators LPEC. Let us consider the effect of ECE (p=3), made in the form of a thin copper disk with an axial height H_3=1 mm, whose radial dimensions are equal to the same dimensions of the WI and WA, the established distance Δz_{13}=(2.5 ... 10.0) mm from the WI.

When WI is excited from the CESD, the currents in the active elements change according to the vibration-damping law. If the disk ECE is located at a distance Δz_{13}=2.5 mm from the WI, then the maximum current densities are: in the WI j_{1m}=893.8 A/mm^2, in the WA j_{2m}=1548.2 A/mm^2, in the ECE j_{3m}=3320,1 A/mm^2 (Fig. 2, *a*). In this case, the EDF f_{zm}=66.97 kN and the EDF F_z=9.6 N·s. The electrodynamic forces are in the nature of almost two consecutive pulses, and the amplitude of the second pulse is significantly lower than the amplitude of the first, both because of a decrease in currents and because of a weakening of the magnetic coupling between the WA and WI. The speed of the armature together with the actuating element is v_2=21 m/s, which determines the efficiency of the converter η=8.95%. During the operation of the LPEC, the active elements are heated to the end of the working cycle. The smallest temperature rise occurs in WI θ_1=0.75ºC, stronger in WA θ_2=1.7ºC and the highest in ECE θ_3=19.0ºC.

When the disk ECE is removed from the WI by a distance of Δz_{13}=10 mm compared to the option considered above (Δz_{13}=2.5 mm), the period of damped current oscillations increases. In this case, the following changes in the performance of the LPEC are occurring (Fig. 2, *b*). The maximum current density in the WI j_{1m} decreases by 15.8%, while the maximum current density in the WA j_{2m}, on the contrary, increases by 4.7%. There is a significant (93.4%) decrease in the maximum current density in the energy efficiency j_{3m}.. Due to this change in currents in the active elements EDF f_{zm} increases by 6.7% and the EDF F_z increases by 18.6%. The increase in power indicators determines the increase in the speed of the armature together with the actuating element v_2 by 18.6%. As a result of this, the efficiency of the converter η increases by 40.6%. A change in current loads causes a change in the heating temperature of the active elements by the end of the working cycle. The temperature rise of the WI θ_1 decreases by 13.6%, the temperature rise of the WA θ_2 increases by 29.4% and, importantly, there is a significant (3.13 times) decrease in the temperature rise of the ECE θ_3.

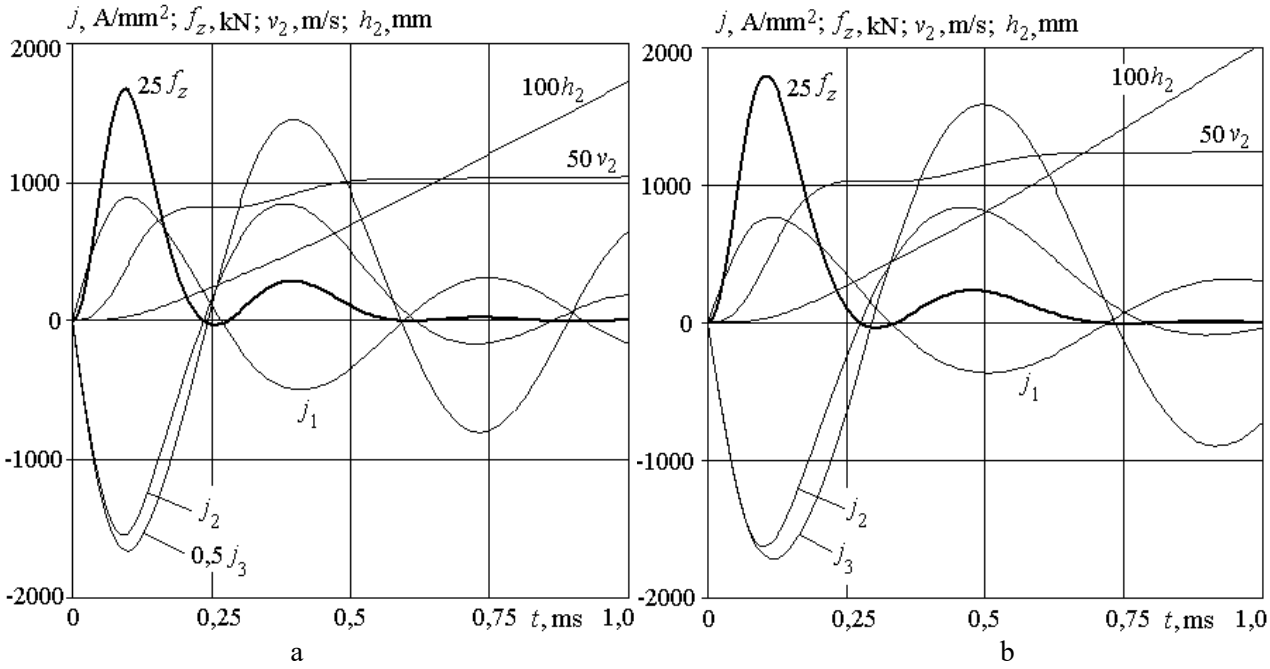

Fig. 2

Figure 3 shows the dependence of the main performance indicators of the LPEC on the relative value of the axial displacement of the disk ECE from the WI $\Delta z_{13}^{*} = \Delta z_{13} / H_1$. An almost monotonous change in the main LPEC indicators in the range $\Delta z_{13}^{*} \subset (0{,}25...1{,}0)$ can be noted. An exception is the behavior of the efficiency η, which varies significantly in the range $\Delta z_{13}^{*} \subset (0{,}25...0{,}5)$, while in the range $\Delta z_{13}^{*} \subset (0{,}5...1{,}0)$ it practically does not change.

Consider the influence of the axial height H_3 of the disk ECE on the main indicators of the LPEC when it is located at a distance $\Delta z_{13}^{*} = 0{,}1$ from the WI. Fig. 4 shows the dependences of the main LPEC indicators on the relative height of the disk ECE $H_3^{*} = H_3 / H_1$. With an increase in the parameter H_3^{*} from 0.05 to 0.2, the maximum current density in theWI j_{1m} decreases by 5.3%, the maximum current density in the WA j_{2m} decreases by 1.7%. Thus there is a significant (3.2 times) reduction in the maximum current density in ECE j_{3m}. Due to this change in currents of the active elements EDF f_{zm} decreases slightly (by 1.9%), while the EDF F_z increases to a greater extent (by 28.8%). An increase EDF F_z causes an increase in the speed of the armature together with the executive element v_2 by 29.8%, which in turn leads to a significant increase in the efficiency of the converter η (by 68.5%). The change in current loads causes a significant change in the heating temperature of the active elements by the end of the working cycle. The temperature rise of the WI θ_1 increases by 2 times, the temperature rise of the WA θ_2 increases by 53.8% and the temperature rise of the ECE θ_3 decreases many-times (5.9 times).

Let us evaluate the effect of the average diameter of an ECE made in the form of a thin (H_3=1 mm) ring with a width $\Delta d_3 = 0{,}5(D_{3ex} - D_{3in})$=10 mm. The relative value of the average diameter of the ring ECE is presented in the form $d_3^{*} = 0{,}5(D_{3ex} + D_{3in}) / D_{1ex}$. Fig. 5 shows the dependences of the main indicators of the LPEC on the value d_3^{*} of the ECE when it is located at a distance $\Delta z_{13}^{*} = 0{,}1$ relative to the WI.

As follows from the presented calculation results, with a decrease in the average diameter of the ring ECE in the range $d_3^{*} \subset (0{,}9...0{,}5)$, the maximum current density slightly decreases in the WI j_{1m} and increases in the WA j_{2m}. However, the maximum current density in ECE has the largest value j_{3m}=5.78 kA/mm^2 with an average value of its diameter (d_3^{*}=0.7). With such a diameter, the following values are provided: armature speed v_2=20.4 m/s, EDF f_{zm}=73 kN, EDF F_z=9.25 N·s and efficiency η=8.31%. But with an average value of the ECE diameter (d_3^{*}=0.7), the excess of its temperature is the largest θ_3=46.6ºC. Thus, it is a ring ECE with an average diameter value d_3^{*}=0.7 that most negatively affects the performance of the LPEC.

Let us consider the effect of the arrangement of the ECE made in the form of a thin-walled ($D_{3ex} = D_{3in} + 2$ mm) cylinder with an axial height H_3=H_1, installed outside the WI and WA with an inner diameter $D_{3in} = D_{1ex} + 2$ mm. Fig. 6 shows the effect of the relative value of the axial displacement of the cylindrical ECE from the WI Δz_{13}^* on the LPEC indicators. The most strongly ECE affects the performance of the LPEC when it is located opposite the WI (Δz_{13}^* = 0.9 ... 1.1). With this arrangement of the cylindrical ECE, the largest values of the maximum current density in the WI j_{1m}=823 A/mm^2 and in the ECE j_{3m}=3.93 kA/mm^2 appear, but the lowest values EDF F_z= 9.38 N·s, the armature speed v_2=20,77 m/s and efficiency η=8.54%. In this case, the temperature rise of the WI is minimum θ_1=0.6ºC and the temperature rise of the ECE is maximum θ_3=22.9ºC.

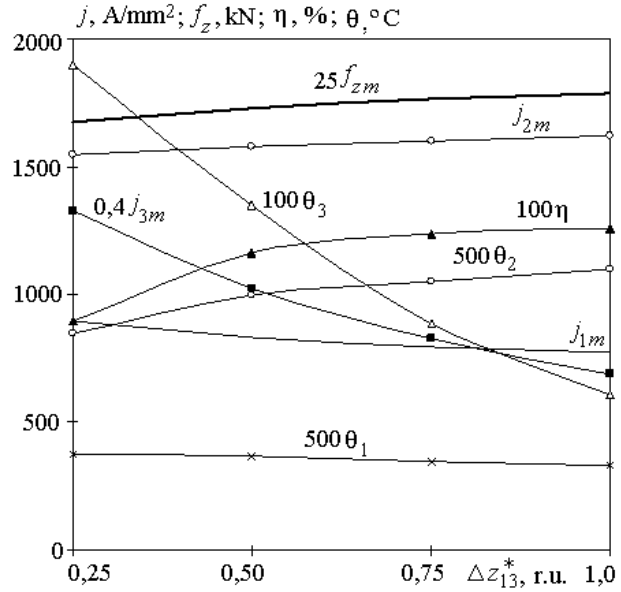

Fig. 3

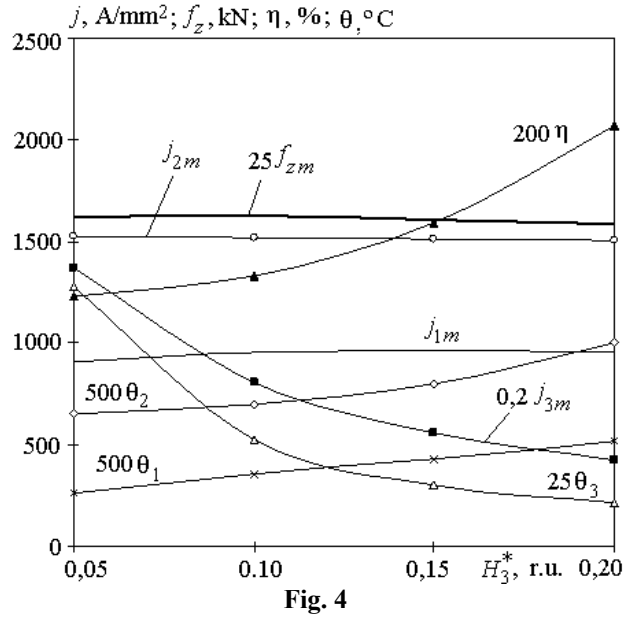

Fig. 4

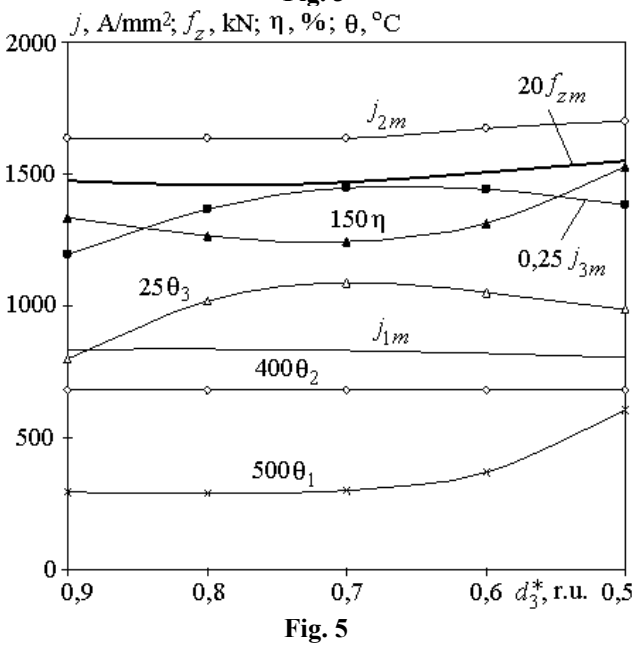

Fig. 5

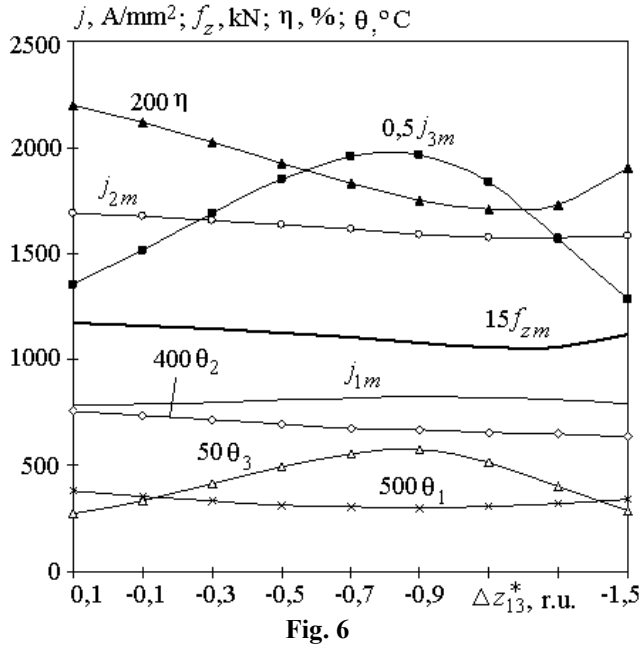

Fig. 6

Thus, the electrically conductive element coaxially installed near the WI has a negative effect on the performance of the induction-type LPEC. The lowest value of the converter efficiency η=6.1% arises when using ECE in the form of a thin copper disk with a height of H_3=0.5 mm, in which the radial dimensions are similar to the dimensions of the WI and WA installed at a minimum distance from the WI Δz_{13}=1.0 mm. For such ECE the temperature excess at the end of the working cycle is maximum θ_3=51ºC. With increasing

thickness of the disk ECE, as well as when it is removed from the WI, the efficiency of the converter increases, and the heating temperature of the ECE decreases. So, when a disk ECE with a height of H_3=1.0 mm is removed by a distance Δz_{13}=10 mm from the WI of the converter efficiency η=12.6%, and its temperature excess is θ_3=6ºC.

Conclusions. 1. A mathematical model has been developed using the lumped parameters of active elements, which describes the interconnected electromechanical and thermal processes in an induction-type LPEC in the presence of a coaxially installed ECE.

2. It was found that the electrically conductive element, coaxially located near the inductor winding, has a negative effect on the performance of the LPEC.

3. The highest value of the converter efficiency of 12.6% occurs when the disk ECE is removed at a significant (over 10 mm) distance from the inductor winding. In this case, the excess temperature ECE is minimal.

4. When the disk ECE approaches the inductor winding and its thickness decreases, the efficiency of the converter decreases, and the excess of the ECE temperature rises. The smallest value of the converter efficiency of 6.1% occurs when EE is used in the form of a thin copper disk 0.5 mm thick, in which the radial dimensions are similar to the sizes of the windings of the inductor and the armature installed at a distance of 1.0 mm from the inductor. In this case, the excess of the ECE temperature is 51ºC.

The work was done on the state budget theme "Improvement of technical systems and devices due to impulse electromechanical converters and electrophysical technologies". State Registration Number: 0117U004881. (01/01/2017 - 31/12/2018).

1. Angquist L., Baudoin A., Norrga S. et al. Low-cost ultra-fast DC circuit-breaker: Power electronics integrated with mechanical switchgear. IEEE International Conference *on Industrial Technology (ICIT)*. Lyon. 2018. Pp. 1708-1713. DOI**:** https://doi.org/10.1109/ICIT.2018.8352439.
2. Bissal A., Magnusson J., Engdahl G. Comparison of two ultra-fast actuator concept. *IEEE Transactions on Magnetics*. 2012. Vol. 48. No 11. Pp. 3315-3318. DOI: https://doi.org/10.1109/tmag.2012.2198447.
3. Soda R., Tanaka K., Takagi K., Ozaki K. Simulation-aided development of magnetic-aligned compaction process with pulsed magnetic field. *Powder Technology*. 2018. Vol. 329. No 15. Pp. 364-370. DOI: https://doi.org/10.1016/j.powtec.2018.01.035.
4. Bolyukh V.F., Dan'ko V.G., Oleksenko S.V. The effect of an external shield on the efficiency of an induction-type linear-pulse electromechanical converter. *Russian Electrical Engineering***.** 2018. Vol. 89. Issue 4. Pp. 275–281. DOI**:** https://doi.org/10.3103/S106837121804003X. (Rus)
5. Bolyukh V.F., Katkov I.I. Cryogenic cooling system "Krioblast" increased efficiency and lowered the operation time of protective electrical induction-induced devices. *ASME International Mechanical Engineering Congress and Exposition*. San Diego, CA, US. 15-21 November 2013. Vol. 8B. Code 105847. Pp. V08BT09A003. DOI: https://doi.org/10.1115/IMECE2013-62383.Bolyukh V.F., Vinnichenko A.I. Concept of an induction-dynamic catapult for a ballistic laser gravimeter. *Measurement Techniques*. 2014. Vol. 56. Issue 10. Pp. 1098-1104. DOI: https://doi.org/10.1007/s11018-014-0337-z. (Rus)
7. Go B.-S., Le D.-V., Song M.-G. et al. Design and electromagnetic analysis of an induction-type coilgun system with a pulse power module. *IEEE Transactions on plasma science*. 2019. Vol. 47, No. 1. Pp. 971–976. DOI: https://doi.org/10.1109/TPS.2018.2874955.
8. Gorodzha K.A., Podoltsev O.D., Troshchinsky B.A. Electromagnetic processes in a pulsed electrodynamic emitter for the excitation of elastic vibrations in concrete structures. *Tekhnichna Elektrodynamika*. 2019. No 3. Pp. 23-28. DOI: https://doi.org/10.15407/techned2019.03.023. (Ukr)
9. Kondratenko I.P., Zhiltsov A.V., Paschin M.O., Vasyuk V.V. Choice of parameters of induction electromechanical converter for electrodynamic processing of welded joints. *Tekhnichna Elektrodynamika*. 2017. No 5. Pp. 83-88. DOI: https://doi.org/10.15407/techned2017.05.083. (Ukr)
10. Kondratiuk M., Ambroziak L. Concept of the magnetic launcher for medium class unmanned aerial vehicles designed on the basis of numerical calculations. *Journal of Theoretical and Applied Mechanics*. 2016. Vol. 54, Issue 1. Pp. 163-177. DOI: https://doi.org/10.15632/jtam-pl.54.1.163.
11. Lim D.K., Woo D.K., Kim I.W. Characteristic analysis and design of a Thomson coil actuator using an analytic method and a numerical method. *IEEE Transactions on Magnetics*. 2013. Vol. 49. No. 12. Pp. 5749–5755. URL: https://www.ingentaconnect.com/content/iee/00189464/2013/00000049/00000012/art00024;jsessionid=1jo2grl3onerq.x-ic-live-03
12. Vilchis-Rodriguez D.S., Shuttleworth R., Barnes M. Modelling thomson coils with axis-symmetric problems: practical accuracy considerations. *IEEE Transactions on Energy Conversion*. 2017. Vol. 32. No. 2. Pp. 629-639. DOI: https://doi.org/10.1109/TEC.2017.2651979.

13. Bach Ju., Bricquet C. Electric switching device with ultra-fast actuating mechanism and hybrid switch comprising one such device. *US Patent* 8686814, H01H77/00. Assignee: Schneider Electric Industries SAS. 01.04.2014.
14. Zhou Y., Huang Y., Wen W. et al. Research on a novel drive unit of fast mechanical switch with modular double capacitors. *Journal of Engineering*. 2019. Vol. 2019. Issue 17. Pp. 4345-4348. DOI: https://doi.org/10.1049/joe.2018.8148.

ВЛИЯНИЕ ЭЛЕКТРОПРОВОДНОГО ЭЛЕЛЕНТА НА ПОКАЗАТЕЛИ ИМПУЛЬСНОГО ЭЛЕКТРОМЕХАНИЧЕСКОГО ПРЕОБРАЗОВАТЕЛЯ ИНДУКЦИОННОГО ТИПА

В.Ф. Болюх, докт. техн. наук
Национальный технический университет «Харьковский политехнический институт»,
ул. Кирпичева, 2, Харьков, 61002, Украина, e-mail: vfbolyukh@gmail.com

Целью статьи является исследование влияния геометрических параметров и расположения коаксиально расположенного электропроводящего элемента (ЭЭ), выполненного в виде тонкостенного диска, кольца или полого цилиндра, на характеристики и показатели линейного импульсного электромеханического преобразователя (ЛИЭП) индукционного типа. Разработана математическая модель, которая описывает электромеханические и тепловые процессы в ЛИЭП индукционного типа с использованием сосредоточенных параметров активных элементов. Показано, что ЭЭ, коаксиально установленный вблизи обмотки индуктора, оказывает негативное влияние на показатели ЛИЭП. Наименьшее значение КПД преобразователя 6,1 % возникает при использовании ЭЭ в виде тонкого медного диска высотой 0,5 мм, у которого радиальные размеры аналогичны размерам обмоток индуктора и якоря, установленного на минимальном расстоянии от индуктора. При этом превышение температуры электропроводящего элемента максимально и равно 51°С. При увеличении толщины ЭЭ и его удалении от индуктора КПД ЛИЭП повышается, а превышение температуры ЭЭ снижается. При удалении дискового ЭЭ высотой 1,0 мм на расстояние 10 мм от индуктора КПД ЛИЭП равно 12,6%, а превышение температуры ЭЭ равно 6°С. Библ. 14, рис. 6.

Ключевые слова: линейный импульсный электромеханический преобразователь индукционного типа, электропроводящий элемент, математическая модель, электромеханические и тепловые процессы и показатели.

УДК 621.313:536.2.24:539.2

ВПЛИВ ЕЛЕКТРОПРОВІДНОГО ЕЛЕМЕНТУ НА ПОКАЗНИКИ ЛІНІЙНОГО ІМПУЛЬСНОГО ЕЛЕКТРОМЕХАНІЧНОГО ПЕРЕТВОРЮВАЧА ІНДУКЦІЙНОГО ТИПУ

В.Ф. Болюх, докт. техн. наук
Національний технічний університет «Харківський політехнічний інститут»,
вул. Кирпичова, 2, Харків, 61002, Україна, e-mail: vfbolyukh@gmail.com

Метою статті є дослідження впливу геометричних параметрів і розміщення коаксиально розташованого електропровідного елементу (ЕЕ), виконаного у вигляді тонкостінного диску, кільця або порожнистого циліндру на характеристики та показники лінійного імпульсного електромеханічного перетворювача (ЛІЕП) індукційного типу. Розроблено математичну модель, яка описує електромеханічні та теплові процеси в ЛІЕП індукційного типу з використанням зосереджених параметрів активних елементів. Показано, що ЕЕ, який коаксіально встановлений поблизу обмотки індуктора, здійснює негативний вплив на показники ЛІЕП. Найменше значення ККД перетворювача 6,1% виникає у разі використання ЕЕ у вигляді тонкого мідного диску висотою 0,5 мм, у якого радіальні розміри аналогічні розмірам обмоток індуктора та якоря, встановленого на мінімальній відстані від індуктора. У цьому разі перевищення температури ЕЕ максимальне і дорівнює 51°С. За збільшенням товщини ЕЕ та його віддалені від індуктора ККД ЛІЕП підвищується, а перевищення температури ЕЕ зменшується. У разі віддаленя дискового ЕЕ висотою 1,0 мм на відстань 10 мм від індуктора КПД ЛІЕП дорівнює 12,6%, а перевищення температура ЕЕ – 6°С. Бібл. 14, рис. 6.

Ключові слова: лінійний імпульсний електромеханічний перетворювач індукційного типу, електропровідний елемент, математична модель, електромеханічні та теплові процеси та показники.

Роботу виконано за держбюджетною темою «Удосконалення технічних систем та пристроїв за рахунок імпульсних електромеханічних перетворювачів та електрофізичних технологій». Номер державної реєстрації: 0117U004881.

Надійшла 10.02.2020
Остаточний варіант 16.03.2020